THE JOURNAL OF BIOLOGICAL CHEMISTRY VOL. 287, NO. 11, pp. 8652–8659, March 9, 2012

Characterization and Purification of a Na^+/Ca^{2+} Exchanger from an Archaebacterium*

Received for publication, December 6, 2011, and in revised form, January 9, 2012 Published, JBC Papers in Press, January 27, 2012, DOI 10.1074/jbc.M111.331280

Gabriel Mercado Besserer[‡], Debora A. Nicoll[‡§], Jeff Abramson[‡1], and Kenneth D. Philipson[‡§2]

From the [‡]Department of Physiology and the [§]Cardiovascular Research Laboratories, David Geffen School of Medicine at UCLA, Los Angeles, California 90095-1751

Background: Databases include many putative prokaryotic Na^+/Ca^{2+} exchangers, but none have been functionally expressed.
Results: A membrane protein (MaX1) of *Methanosarcina acetivorans* catalyzes electrogenic countertransport of Na^+ and Ca^{2+}.
Conclusion: MaX1 has properties similar to those of mammalian Na^+/Ca^{2+} exchangers.
Significance: The characterization and purification of MaX1 should facilitate structure/function studies.

The superfamily of cation/Ca^{2+} exchangers includes both Na^+/Ca^{2+} exchangers (NCXs) and Na^+/Ca^{2+},K^+ exchangers (NCKX) as the families characterized in most detail. These Ca^{2+} transporters have prominent physiological roles. For example, NCX and NCKX are important in regulation of cardiac contractility and visual processes, respectively. The superfamily also has a large number of members of the YrbG family expressed in prokaryotes. However, no members of this family have been functionally expressed, and their transport properties are unknown. We have expressed, purified, and characterized a member of the YrbG family, MaX1 from *Methanosarcina acetivorans*. MaX1 catalyzes Ca^{2+} uptake into membrane vesicles. The Ca^{2+} uptake requires intravesicular Na^+ and is stimulated by an inside positive membrane potential. Despite very limited sequence similarity, MaX1 is a Na^+/Ca^{2+} exchanger with kinetic properties similar to those of NCX. The availability of a prokaryotic Na^+/Ca^{2+} exchanger should facilitate structural and mechanistic investigations.

The Na^+/Ca^{2+} exchangers are plasma membrane proteins that have important roles in maintaining Ca^{2+} homeostasis in nearly all types of animal cells (1). Na^+/Ca^{2+} exchangers function as efficient electrogenic antiporters that extrude cytoplasmic Ca^{2+} against an electrochemical potential by utilizing the energy of the inwardly directed Na^+ gradient. The two primary groups of Na^+/Ca^{2+} exchangers are the K^+-independent and K^+-dependent Na^+/Ca^{2+} exchangers (NCX[3] and NCKX families, respectively). NCXs exchange 3 Na^+ for 1 Ca^{2+} (although this stoichiometry is not absolute) (2), whereas NCKXs exchange 4 Na^+ for 1 Ca^{2+} plus 1 K^+. The Na^+/Ca^{2+} exchangers are identified by regions known as α repeats (3), which define the superfamily. The α repeats (α-1 and α-2) are regions of intramolecular homology within the TMSs (see Fig. 1) that are important for transport function (4, 5), *i.e.* α repeats of members of the exchanger family demonstrate both inter- and intramolecular homology.

Na^+/Ca^{2+} exchange activity has critical roles in cardiac contractility, smooth muscle tone, renal Ca^{2+} reabsorption, photoreceptor signal transduction, and neural function. NCX1.1 of cardiac muscle is the Na^+/Ca^{2+} exchanger that has been investigated in most detail. This includes functional, structural, and physiological studies (1, 6, 7). The Na^+/Ca^{2+},K^+ exchanger of rod photoreceptors, NCKX1, has also received much attention (8).

The animal NCX and NCKX proteins are members of a larger cation/Ca^{2+} exchanger superfamily (9), which consists of five discrete clade groups of structural homologs. The other groups of the superfamily include the insect and nematode cation/Ca^{2+} exchangers (CCX), the plant and fungi H^+/Ca^{2+} exchangers (CAX), and the archaeal and eubacterial YrbG group (named after the gene of the homolog found in *Escherichia coli*), for which no known function for any member has been described. The YrbG homologs are of special interest, as prokaryotic membrane proteins have the potential of being more experimentally tractable than eukaryotic exchangers for many studies. There have been a few sporadic reports in the literature of prokaryotic Na^+/Ca^{2+} exchange activity in membranes from a *Halobacterium* (10), an alkalophilic *Bacillus* (11), and *Streptococcus pneumoniae* (12). In no case, however, has the exchange activity been associated with a specific protein.

Current information from completely sequenced genomes of bacteria and archaea has revealed the existence of many YrbG-related genes with characteristic α repeats. We expressed several of these genes in *E. coli*. One of these genes from the archaeon *Methanosarcina acetivorans* expressed well and was amenable to purification and reconstitution. We report here the functional characterization of the *M. acetivorans* NCX homolog (MaX1), the first known prokaryotic Na^+/Ca^{2+} exchanger protein.

EXPERIMENTAL PROCEDURES

Reagents—All reagents were of the highest purity available commercially. Valinomycin was from Sigma-Aldrich; DDM

* This work was supported, in whole or in part, by National Institutes of Health Grants R01 HL49101 (to K. D. P.) and R21 HL093278 (to J. A.).
[1] To whom correspondence may be addressed. E-mail: jabramson@mednet.ucla.edu.
[2] To whom correspondence may be addressed. Tel.: 310-825-7679; Fax: 310-206-5777; E-mail: kphilipson@mednet.ucla.edu.
[3] The abbreviations used are: NCX, Na^+/Ca^{2+} exchanger; NCKX, Na^+/Ca^{2+},K^+ exchanger; TMS, transmembrane segment; DDM, *n*-dodecyl-β-D-maltoside; HRV, human rhinovirus; GpA, glycophorin A; ISO, inside-out; PMSF, phenylmethylsulfonyl fluoride.

was from Anatrace; *Taq* polymerase and restriction enzymes were from New England Biolabs; and the protein ladder was from Fermentas. *E. coli* strains were obtained from Stratagene. Growth media were from VWR International. PCR primers were obtained from Integrated DNA Technologies.

Bacteria, Plasmids, and Growth Media—The LB plates contained Luria broth (13) plus 15 g/liter Bacto agar (VWR International). Terrific broth medium contained 12 g/liter Bacto-Tryptone (VWR International), 24 g/liter Bacto-yeast extract (VWR International), 4 ml/liter glycerol, 2.3 g/liter KH_2PO_4, and 12.5 g/liter K_2HPO_4. Kanamycin antibiotic (Sigma) was added to the media at 50 μg/ml. Cloning and propagation of DNA were done in *E. coli* XL1-Blue cells (Stratagene), and the *E. coli* C41(DE3) strain was used for expression of MaX1 (14).

Construction of MaX1-pWarf—The gene encoding MaX1 was amplified by PCR from purified *M. acetivorans* genomic DNA using oligomers GACACTCGAGATGATCACAGTGAATTTTCTCATTC and GAACGGATCCGATGTAGAATAAAACTACAAGG, designed from the Q8TPA6 genome sequence (UniProt). The isolated amplified product was cloned into the XhoI-BamHI sites of the pWarf(+) or pWarf(−) vectors (15) using standard restriction and ligation techniques. Constructs were verified by sequencing. Cloning MaX1 into pWarf vectors allows MaX1 to be fused at its C terminus to a HRV 3C protease tag followed by a GFP reporter fusion protein and a His_8 tag, which allows for experimental manipulation. When cleaved with HRV 3C, MaX1 is liberated from the rest of the fusion tag, producing full-length MaX1 with a 6-amino acid overhang as described by Hsieh *et al.* (15). pWarf(+) has an additional sequence representing the TMS of GpA between the HRV 3C site and GFP. A MaX1-His construct was also prepared by mutating the HindIII site of pWarf(+) into a BamHI site, digesting the resulting construct with BamHI to excise the HRV 3C-GpA-GFP tag, and then re-ligating the construct.

Growth and Expression Conditions—MaX1 was expressed under optimized conditions as follows. 50 ml of LB medium in 250-ml baffled flasks was inoculated with freshly transformed C41(DE3) colonies carrying the MaX1-pWarf(+) construct or the empty pWarf(+) vector as a control and grown overnight at 37 °C and 225 rpm. 10 ml of the overnight cultures was diluted into 1 liter of Terrific broth medium in 4-liter baffled flasks and incubated at 37 °C and 225 rpm until the absorbance at 600 nm reached 0.8. At this point, the temperature was lowered to 25 °C, and fusion protein expression was induced for 6 h with 1 mM isopropyl β-D-thiogalactopyranoside. Cells were then harvested by low speed centrifugation and stored at −20 °C.

Isolation of Inside-out Membrane Vesicles—Cells were harvested at 5500 rpm for 10 min at 4 °C and washed with 50 mM potassium P_i (pH 7.5). ISO bacterial membrane vesicles were prepared using the methodology of Nagamori *et al.* (16). The final ISO vesicle pellet was resuspended in 50 mM potassium P_i and 1 mM EDTA, homogenized, and flash-frozen to −80 °C for storage. The protein concentration was determined by the BCA protein assay (Pierce). The presence of MaX1 in the ISO vesicles was verified by Western blotting using HRP-conjugated anti-pentahistidine antibody (Qiagen) and visualized by a horseradish peroxidase reaction and in-gel GFP fluorescence (17).

Detergent Solubilization and Purification—Cell pellets containing the overexpressed MaX1-GFP fusion protein were resuspended in 5 ml of lysis buffer (50 mM Tris (pH 7.5), 150 mM NaCl, 0.04 mg/ml DNase, and 0.1 mM PMSF) per g of cells and disrupted using an EmulsiFlex C3 system (ATA Scientific). Cell debris was removed by low speed centrifugation at 10,000 × *g* for 20 min, and membranes were isolated by ultracentrifugation at 302,000 × *g* for 1 h. All steps were performed at 4 °C.

Membranes were solubilized in 50 mM Tris (pH 8), 150 mM NaCl, 20 mM imidazole, and 2% DDM at 4 °C with continuous stirring for 1 h. Membrane debris was cleared by centrifugation at 53,000 × *g* for 1 h. Solubilized MaX1-GFP from the supernatant was then purified to homogeneity by immobilized metal ion affinity chromatography using a nickel-nitrilotriacetic acid Superflow resin column (Qiagen). The column was washed with 50 mM Tris (pH 8), 150 mM NaCl, 25 mM imidazole, and 0.017% DDM for 20 column volumes and eluted in a linear gradient from 25 to 500 mM imidazole over 10 column volumes at a flow rate of 1.0 ml/min.

Eluted fractions were concentrated and washed with 50 mM Tris (pH 7.5) and 50 mM NaCl using 100-kDa Amicon concentrators with centrifugation at 12,000 × *g* for 30 min. Enriched MaX1 proteins were adjusted to 10 mg/ml in 50 mM Tris (pH 7.5), 50 mM NaCl, 0.017% DDM, and 50% glycerol buffer and stored at −80 °C.

Samples were examined on SDS-9% polyacrylamide gels stained with Coomassie Blue, and protein concentration was determined at A_{280} using extinction coefficients of 50,895 M^{-1} cm^{-1} for MaX1-GpA-GFP-His and 28,880 M^{-1} cm^{-1} for MaX1-His (ProtParam).

Activity Assays—Frozen ISO bacterial vesicles were resuspended in a 100-fold excess volume of 140 mM NaCl and 10 mM MOPS/Tris (pH 7.4) and incubated at 4 °C for 1 h. Vesicles were then recovered by ultracentrifugation at 140,000 × *g* for 90 min. Pellets were resuspended in 140 mM NaCl and 10 mM MOPS/Tris (pH 7.4) to a final concentration of 5 mg/ml total protein and incubated at 4 °C for at least 4 h. In some cases, we used KCl, LiCl, or choline chloride as a substitute for NaCl to prepare vesicles loaded with ions other than Na^+.

Na^+ gradient-dependent $^{45}Ca^{2+}$ uptake was measured as described in detail previously (18). Typically, 5 μl of NaCl (140 mM)-loaded *E. coli* vesicles was rapidly added to 245 μl of Ca^{2+} uptake medium containing 140 mM choline chloride, 10 mM MOPS/Tris (pH 7.4), 10 μM $CaCl_2$, and 6 μCi/ml $^{45}CaCl_2$ at 37 °C. Variations of this protocol are noted below.

The Ca^{2+} uptake reaction was stopped after 5 s by the automated addition of 30 μl of 140 mM KCl and 10 mM EGTA. Immediately thereafter, 1 ml of ice-cold 140 mM KCl and 1 mM EGTA was added. 1 ml of this solution was applied to a 0.45-μm Millipore nitrocellulose filter under suction. The filter was washed with two 3-ml aliquots of ice-cold 140 mM KCl and 1 mM EGTA. Radioactive Ca^{2+} on the filters was quantified by liquid scintillation counting. Data are shown as means ± S.E.

RESULTS AND DISCUSSION

Prokaryotic YrbG Homologs—We cloned 12 YrbG homologs using PCR products from genomic DNA. The clones were

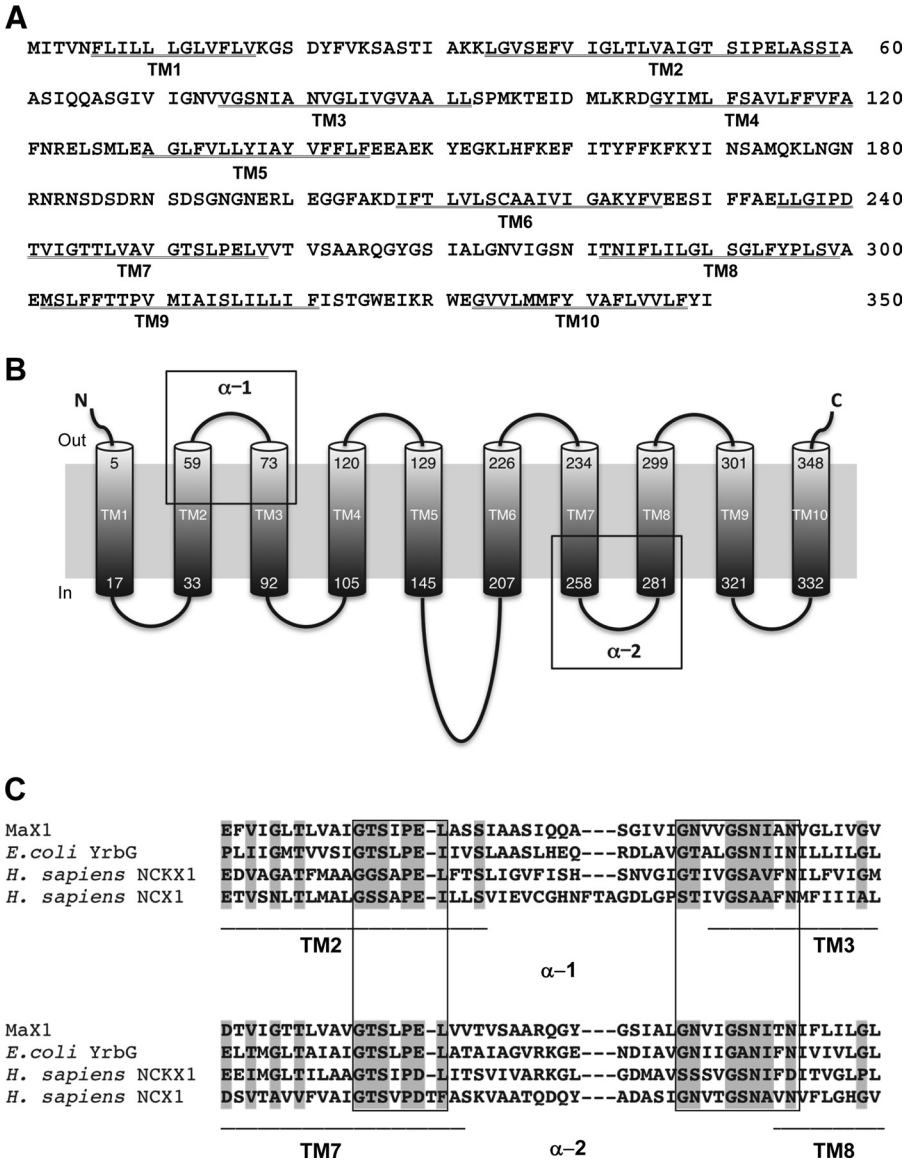

FIGURE 1. **MaX1 protein.** *A*, sequence and proposed TMSs (*TM*; *double underlines*) of MaX1. *B*, proposed secondary structure of MaX1. Note the opposite orientations of the homologous α repeats. The *numbers* inside each putative TMS indicate beginning and ending residues. *C*, ClustalW sequence alignment of the highly conserved α-1 and α-2 repeats of MaX1 with those from a putative *E. coli* NCX (YrbG) and from human NCKX1 and NCX1. Highly conserved amino acids are highlighted in *gray*, and two highly conserved and internally homologous regions are *boxed*.

inserted into both pWarf(+) and pWarf(−) expression vectors (15) and expressed in *E. coli*. In initial studies, we found that the YrbG homolog from the archaeon *M. acetivorans* (MaX1) expressed well, displayed functional activity, and could be purified. We chose to concentrate on MaX1 (UniProt Q8TPA6) for initial characterization of a member of the YrbG family.

MaX1 Sequence Analysis—The MaX1 open reading frame is 1050 bp and encodes a protein of 350 amino acids with a calculated molecular mass of 38 kDa. Hydropathy analysis predicted that MaX1 contains 10 TMSs (Fig. 1, *A* and *B*) arranged in two groups of five TMSs separated by a hydrophilic intracellular domain of ~63 amino acids. To model the potential TMSs (Fig. 1*A*), we utilized the results predicted by the TMpred program with the standard prediction parameters for a transmembrane helix length of between 12 and 33 residues, similarities between the two halves of MaX1 (see below), and similarities to NCX1 (19, 20) and YrbG (21), for which TMSs have been experimentally determined. NCX1 has nine TMSs, but like YrbG, MaX1 is predicted to have an additional TMS in the C-terminal half of the protein that places the C terminus at the extracellular surface. The "inside positive" rule (22), that arginine and lysine residues are more prevalent in loops connecting TMSs at the intracellular surface than in extracellular loops, is obeyed in this model for MaX1.

MaX1 contains α repeats (Fig. 1, *B* and *C*), the defining characteristic of Na^+/Ca^{2+} exchangers. These regions span TMS2 and TMS3 (α-1) and TMS7 and TMS8 (α-2) and, for MaX1, are 50% identical (compared with 24% identity between the NCX1 α repeats). For MaX1, as for the putative *E. coli* exchanger YrbG (21), the identities between the two halves of the proteins is striking and is further evidence that the exchanger proteins arose from a gene duplication event. That the α repeats are the

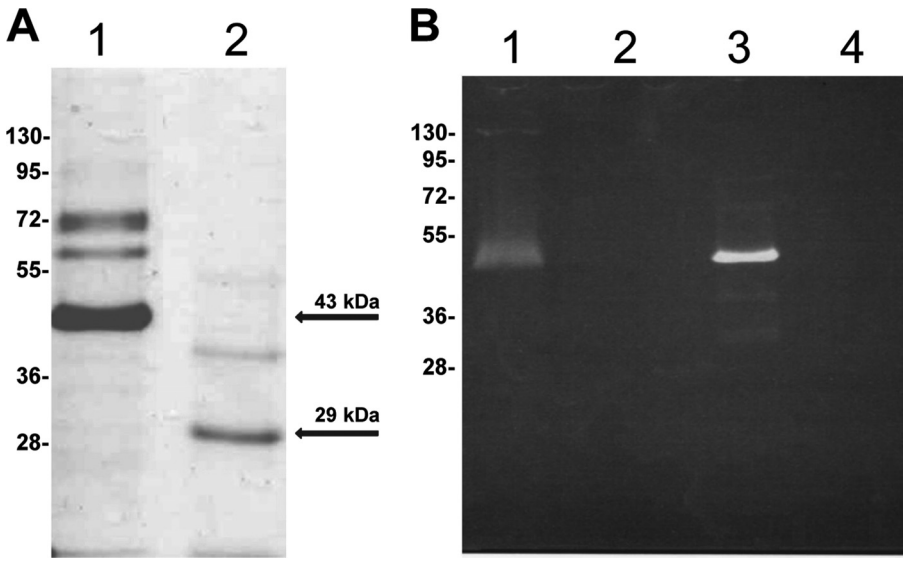

FIGURE 2. **SDS-PAGE analysis of MaX1-GpA-GFP-His_8 and MaX1-His_8 fusion proteins.** *A*, overexpressed MaX1-GpA-GFP-His_8 (*lane 1*) and MaX1-His_8 (*lane 2*) fusion proteins were purified with a nickel affinity column from DDM-solubilized *E. coli* (C41(DE3)) membranes, analyzed by 9% SDS-PAGE, and visualized with Coomassie Brilliant Blue R-250. *Arrows* indicate the positions of MaX1-GpA-GFP-His and MaX1-His_8 fusion proteins. *B*, the identity of MaX1-GpA-GFP-His_8 protein in ISO vesicles (*lane 1*) was confirmed by 9% SDS-PAGE in-gel GFP fluorescence by comparison with ISO vesicles containing overexpressed MaX1-His_8 (*lane 2*) or purified MaX1-GpA-GFP-His_8 (*lane 3*) and MaX1-His_8 (*lane 4*) proteins. 5 μg of protein was loaded per lane. See "Experimental Procedures" for further details.

only part of this gene duplication event still in evidence in the mammalian exchangers strongly suggests the functional importance of these regions and is consistent with mutational analysis (4, 5). In Fig. 1*C*, the MaX1 α repeats are aligned with those from NCX1, NCKX1, and YrbG. MaX1 α-1 is 31% and α-2 is 40% identical to their human NCX1 counterparts. Each of the α repeats maintains the conserved motif G(T/S)S*X*P(E/D)X_{21-24}GSX_3N, which has been implicated in ion transport in NCX1. For example, Asp-54 (α-1 region) and Glu-256 (α-2 region) of MaX1 are homologous to Glu-113 and Asp-814 of NCX1.1. Conservative mutations of Glu-113 and Asp-814 completely inactivate NCX1.1 (5). The α repeats are present on opposite sides of the membrane and likely form an inverted repeat motif, as seen in Na^+ symporters (23).

Like the NCXs, MaX1 has a hydrophilic domain between TMS5 and TMS6 that is modeled to be intracellular. However, in MaX1, this domain is small, only 63 amino acids, with 10 acidic and 11 basic amino acids and a calculated pI of 7. The hydrophilic domain contains neither the exchanger inhibitory peptide (24) nor Ca^{2+} regulatory domains (25, 26) that have been identified in NCXs. A BLASTp search with the hydrophilic domain revealed similarities only to other bacterial members of the NCX superfamily. Thus, there is no evidence that this domain is involved in any specific regulatory role, as it is in the mammalian NCXs.

M. acetivorans has two additional genes with high similarity to MaX1 that we designate MaX2 (GenBank™ accession number NP617716.1) and MaX3 (NP617914.1). MaX1 and MaX2 have an identity of 47%. MaX3 is more divergent, with 29 and 28% identities to MaX1 and MaX2, respectively. The identities are primarily restricted to the TMSs. The hydrophilic domains between TMS5 and TMS6 of the MaX proteins are quite different, and the MaX2 domain is curiously enriched in glutamate, lysine, and isoleucine (22, 15, and 15%, respectively). Because, in NCX1, the TMSs are important in ion transport and the hydrophilic domain is important in regulation, the sequences suggest that the MaX proteins share similar transport properties but different regulatory properties or expression profiles.

Expression and Purification—GFP fluorescence is a useful tool to monitor protein expression and purification, but, if the C terminus of a membrane protein is extracellular, GFP fluorescence is not detected. The pWarf(+) and pWarf(−) expression vectors both fuse a HRV 3C protease site followed by GFP and a His_8 tag to the C terminus of the expressed protein. In addition, there is a sequence representing the TMS of GpA between the HRV 3C site and GFP in pWarf(+).The presence of the additional TMS creates an internal C terminus for those membrane proteins with endogenous external C termini. Expression of MaX1 showed a membrane-associated accumulation of GFP fluorescence only when expressed with pWarf(+) (data not shown), indicating that the C terminus of MaX1 is extracellular. The vector system is described in detail in Ref. 15.

Tagged MaX1 was purified using a nickel affinity column (Fig. 2, *A* and *B*), with a recovery of ~33% and a final yield of ~1 mg/liter of culture medium. The apparent molecular mass of tagged MaX1 is 43 kDa. The higher molecular mass bands may be at least partially due to oligomerization, as they show some signal by in-gel GFP fluorescence. The identity of the protein was verified by confirming the presence of GFP by in-gel fluorescence and mass spectrometry (data not shown). We were also able to isolate a MaX1-His protein lacking the other tags, as shown in Fig. 2.

MaX1 Catalyzes Na^+ Gradient-dependent Ca^{2+} Uptake—In most experiments, we used ISO membrane vesicles from *E. coli* expressing MaX1 tagged (HRV 3C protease site, GpA, GFP, and His tag) at the C terminus. For simplicity, we will refer to this protein as MaX1. Control experiments will be described below to demonstrate that it is unlikely that the presence of these tags,

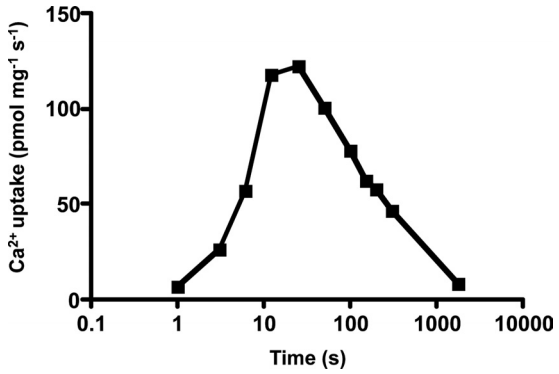

FIGURE 3. **Time course of Ca^{2+} uptake mediated by MaX1.** NaCl (140 mM)-loaded membrane vesicles from *E. coli* expressing MaX1 protein were diluted 50-fold into reaction medium containing choline chloride plus 10 μM $^{45}Ca^{2+}$ and incubated at 37 °C. Aliquots of 250 μl were removed at the indicated times, and $^{45}Ca^{2+}$ uptake was stopped by the addition of 1 ml of cold 140 mM KCl and 1 mM EGTA. Assays were performed in duplicate using three different vesicle preparations. Shown is a representative experiment.

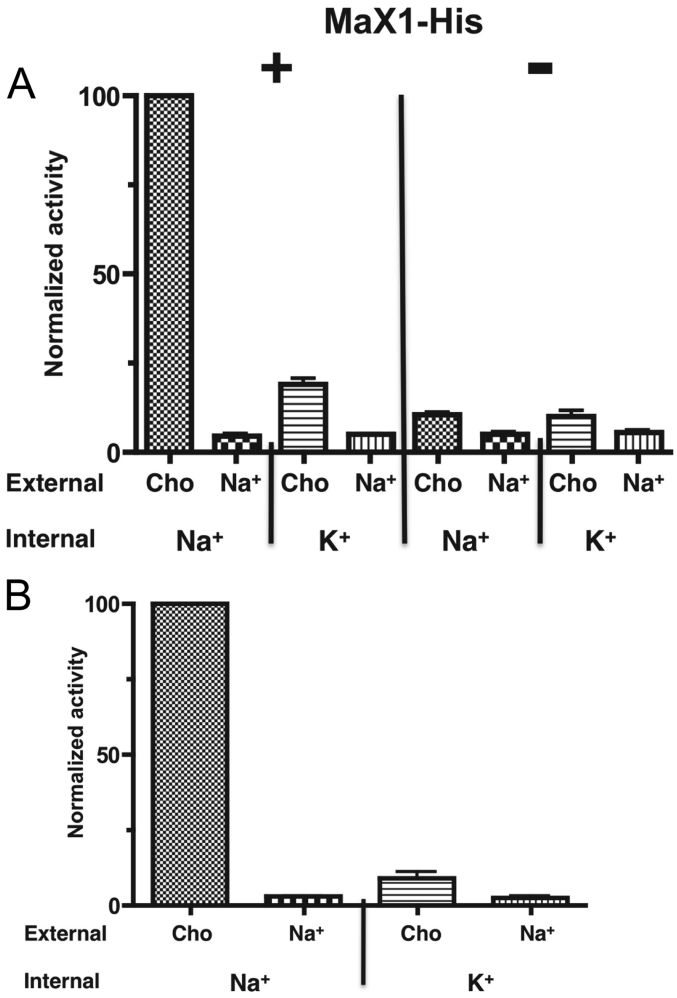

FIGURE 4. **Ionic requirements for Ca^{2+} uptake mediated by MaX1.** *A*, membrane vesicles from *E. coli* expressing MaX1-His protein (*left*) or control vesicles (*right*) with intravesicular NaCl or KCl (140 mM) were diluted 50-fold into reaction medium containing either choline chloride or NaCl (140 mM) plus 10 μM $^{45}Ca^{2+}$. Ca^{2+} uptake was stopped after 5 s. See "Experimental Procedures" for more details. *B*, identical experiments using membrane vesicles expressing the fully tagged MaX1 protein. Assays were performed in duplicate using three different vesicle preparations. Data were normalized to control uptake conditions.

including the additional TMS provided by the GpA, altered transport properties.

To test the possibility that MaX1 functions as a Na^+/Ca^{2+} exchanger, we measured Na^+ gradient-dependent $^{45}Ca^{2+}$ uptake into membrane vesicles. Briefly, Na^+-loaded vesicles were diluted into Na^+-free medium containing $^{45}Ca^{2+}$ to activate Ca^{2+} uptake. This assay has been utilized extensively to investigate mammalian Na^+/Ca^{2+} exchangers (18). Fig. 3 shows the time course of Ca^{2+} uptake into vesicles diluted in choline chloride medium. Several experiments demonstrated that Ca^{2+} uptake was linear for ~10 s. In experiments below, uptake was carried out for 5 s as a measure of the initial rate. Ca^{2+} uptake was maximal at ~1 min and then declined over several minutes to a low level. This time course is important because it demonstrates that Ca^{2+} is accumulating against a concentration gradient and is not merely passively equilibrating across the membrane. Thus, the Ca^{2+} uptake must be driven by an energy source (presumably the Na^+ gradient). After the Na^+ gradient dissipates, accumulated Ca^{2+} leaks out of the vesicles and eventually reaches an equilibrium value. Uptake varied with preparation but was always within the range of 70–90 pmol of Ca^{2+}/mg of protein/s when Ca^{2+} was 10 μM.

In some initial experiments, we used membrane vesicles isolated from *E. coli* expressing MaX1 with only a His tag at the C terminus (MaX1-His). This is the case for the results shown in Fig. 4*A*. To begin characterization of MaX1 function, we measured $^{45}Ca^{2+}$ uptake into MaX1-His membrane vesicles under different ionic conditions (Fig. 4*A*, *left*). Ca^{2+} uptake required the presence of an outwardly directed Na^+ gradient. K^+-loaded (or choline-loaded (data not shown)) vesicles did not facilitate substantial uptake of Ca^{2+}. Intravesicular Na^+ catalyzed Ca^{2+} uptake only if extravesicular Na^+ was absent. Extravesicular Na^+ inhibited Ca^{2+} uptake presumably by competing with Ca^{2+} for binding to transport sites. These properties are characteristic of Na^+/Ca^{2+} exchangers (1). These experiments were repeated using membrane vesicles from *E. coli* not induced to express MaX1 (Fig. 4*A*, *right*). The *E. coli* vesicles not expressing MaX1 did not display significant Ca^{2+} uptake under any ionic conditions. Thus, if *E. coli* expresses a native Na^+/Ca^{2+} exchanger, the level is below that needed for detection in this Ca^{2+} transport assay.

These experiments were repeated using fully tagged MaX1 (Fig. 4*B*). The results were essentially identical to those obtained using MaX1-His (Fig. 4*A*). Although we would have preferred to do all functional studies using native untagged MaX1, this proved to be difficult. First, MaX1-His with only one tag instead of four labels (HRV 3C, GpA, GFP, and His) did not express reproducibly well. Therefore, we performed only some initial experiments with this protein (see Fig. 4*A* and select experiments below). In all tested cases, the results were identical between MaX1-His and fully tagged MaX1. This suggests that the tags were not altering transport properties. Second, we attempted to remove tags from fully tagged MaX1 using HRV 3C protease. However, we found that the cleavage reaction was quite inefficient and thus not practical.

The experiments presented in Fig. 4 demonstrate that the Ca^{2+} uptake facilitated by MaX1 specifically required intrave-

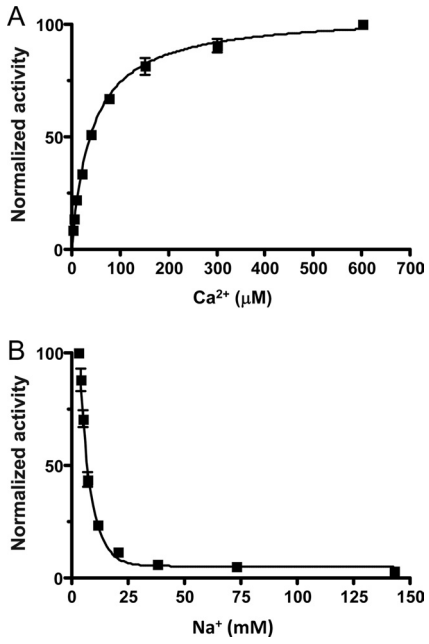

FIGURE 5. **Na^+ and Ca^{2+} concentration dependences for MaX1.** *A*, Na^+ gradient-dependent Ca^{2+} uptake as a function of extravesicular Ca^{2+} concentration. *B*, inhibition of Ca^{2+} uptake by extravesicular Na^+. The Ca^{2+} concentration was 10 μM. All uptakes were terminated after 5 s. Data points are the average of three separate determinations. Data were fit to a single-binding site hyperbolic model (*A*) or to an inverse rectangular hyperbolic model (*B*).

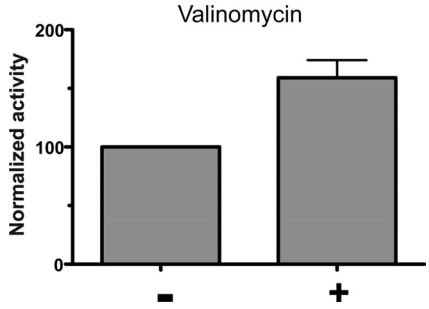

FIGURE 6. **Effects of membrane potential on MaX1-catalyzed Ca^{2+} influx.** Na^+-loaded MaX1 vesicles were diluted into KCl reaction medium in the presence or absence of valinomycin (0.4 μM). Ca^{2+} (10 μM) uptake was stopped after 5 s. Data points are the average of four separate experiments ($p < 0.03$).

sicular Na^+ and the absence of extravesicular Na^+. These characteristics further support the contention that MaX1 is a Na^+/Ca^{2+} exchanger. In single experiments, we found that like K^+, intravesicular choline did not catalyze Ca^{2+} uptake, whereas internal Li^+ induced Ca^{2+} uptake that was slightly higher than that which occurred with internal K^+.

Ca^{2+} and Na^+ Dependences—We measured Na^+ gradient-dependent Ca^{2+} influx as a function of extravesicular Ca^{2+} concentration. Ca^{2+} uptake showed a saturable hyperbolic dependence on Ca^{2+}, with a K_{app} of 41.1 ± 2.0 μM (Fig. 5*A*). Saturation is most consistent with transporter-mediated Ca^{2+} uptake rather than a channel-mediated mechanism. This is a relatively low Ca^{2+} affinity and similar to that displayed by NCX1, which displays an apparent Ca^{2+} affinity of 20–40 μM (27, 28).

We also measured the ability of extravesicular Na^+ to compete with Ca^{2+} for binding to the ion-binding sites. At a constant Ca^{2+} concentration (10 μM), we varied the extravesicular Na^+ concentration. As shown in Fig. 5*B*, external Na^+ was a potent inhibitor of Ca^{2+} uptake ($K_{0.5}$ = 2.9 ± 0.4 mM). In contrast, the $K_{0.5}$ for inhibition of cardiac NCX1 by Na^+ at a Ca^{2+} concentration of 8.6 μM was 12.6 mM (28). The ability of Na^+ to inhibit Ca^{2+} uptake by MaX1 is consistent with the relatively low apparent affinity of MaX1 for Ca^{2+}, enabling potent competition. We have not determined that direct competition is responsible for all of the effects of extravesicular Na^+, *i.e.* we did not examine Na^+ inhibitory potency at other Ca^{2+} concentrations. However, competitive effects are likely to be dominant for a Na^+/Ca^{2+} exchanger. This assertion is supported by studies with other Na^+/Ca^{2+} exchangers (28). We used fully tagged MaX1 to obtain these results. However, a nearly identical result was obtained using MaX1-His ($K_{0.5}$ = 2.2 mM, n = 1).

Na^+/Ca^{2+} Exchange Mediated by MaX1 Is Electrogenic—The NCX transporters exchange 3 Na^+ for each Ca^{2+} (29), although a 4:1 stoichiometry has also been reported (30). Thus, the NCXs are electrogenic, with a net movement of positive charge in the same direction as Na^+ translocation. For NCX1, the electrogenicity is readily demonstrated by using the K^+ ionophore valinomycin to control membrane potential (31). In the absence of valinomycin, the rapid buildup of a negative-inside membrane potential inhibits vesicular Na^+ gradient-dependent Ca^{2+} uptake. Extravesicular K^+/valinomycin prevents the accumulation of intravesicular negative charge and relieves inhibition. To test the effects of membrane potential on MaX1, we measured Ca^{2+} uptake in KCl (140 mM; rather than choline chloride) uptake medium in the presence and absence of valinomycin. Valinomycin stimulated uptake by 60 ± 20% (Fig. 6). The data indicate that MaX1 catalyzes transport with a likely stoichiometry of 3 or more Na^+ for each Ca^{2+}. Valinomycin induced a similar level of stimulation of Ca^{2+} uptake in vesicles expressing MaX1-His (n = 1) (data not shown).

MaX1 could function as a member of the NCKX family, which exchanges 4 Na^+ for 1 Ca^{2+} plus 1 K^+. However, under no circumstances did we observe K^+ stimulation of Na^+/Ca^{2+} exchange activity. Robust Ca^{2+} uptake occurred in the complete absence of K^+. In fact, uptake from high K^+ medium was lower than that from choline medium (see Fig. 7 below).

Cation Inhibition of MaX1 Na^+/Ca^{2+} Exchange—We tested the effects of various cations in the uptake medium on MaX1 Na^+/Ca^{2+} exchange activity at 10 μM Ca^{2+} (Fig. 7). Replacement of choline with equimolar Na^+ eliminated Ca^{2+} uptake, as also seen above (Figs. 4 and 5*B*). Replacement of choline with K^+ or Li^+ reduced Ca^{2+} uptake by 58 and 80%, respectively. Li^+ can substitute for Na^+ on some transporters such as the mammalian Na^+/H^+ exchanger (32) or the mitochondrial Na^+/Ca^{2+} exchanger (33). Cardiac NCX1 does not transport Li^+, although a mutant with altered ion selectivity has been reported to do so (34). Like extravesicular Na^+, Li^+ may compete with Ca^{2+} for transport sites to decrease Ca^{2+} uptake. Possibly, Li^+ is actually transported by MaX1, and Li^+/Ca^{2+} exchange is facilitated. We have not directly tested this possibility.

We next examined inhibition of MaX1 by two divalent cations. At 10 μM Ca^{2+}, Mg^{2+} (5 mM) and Mn^{2+} (1 mM) inhibited Ca^{2+} uptake by 20 ± 7 and 67 ± 2%, respectively. This is some-

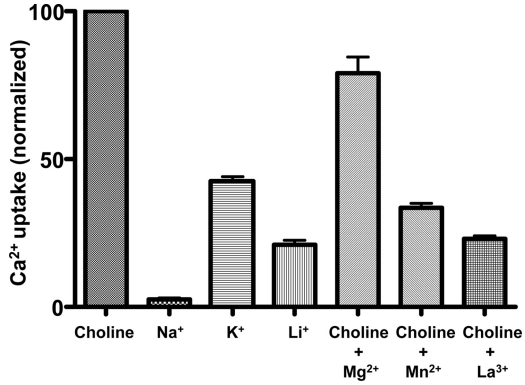

FIGURE 7. **Inhibition of MaX1-mediated Ca^{2+} uptake by mono-, di-, and trivalent cations.** Ca^{2+} uptake was initiated by diluting Na^+-loaded MaX1 vesicles into Ca^{2+} uptake medium containing 140 mM choline chloride, KCl, or LiCl as indicated. When present, the concentrations of $MgCl_2$, $MnCl_2$, and $LaCl_3$ were 5 mM, 1 mM, and 10 μM, respectively. Results are shown as normalized Ca^{2+} uptake ($n = 3$). *Error bars* represent S.E.

what less inhibition than the effects of Mg^{2+} and Mn^{2+} on Ca^{2+} uptake mediated by the cardiac Na^+/Ca^{2+} exchanger (35). The trivalent ion La^{3+} has a similar ionic radius to Ca^{2+} and is often a potent inhibitor of Ca^{2+}-activated events. We found that 10 μM La^{3+} inhibited MaX1 Ca^{2+} uptake by 79 ± 1%. In contrast, La^{3+} inhibited the cardiac sarcolemmal Na^+/Ca^{2+} exchanger with a substantially higher potency. For example, at twice the Ca^{2+} concentration used here, NCX1 was inhibited by almost 100% at 10 μM La^{3+} (35). This suggests that MaX1 and NCX1 do not have identical Ca^{2+}-binding sites.

Conclusions—We describe, for the first time, the functional activity of a member of the YrbG family of the cation/Ca^{2+} exchanger superfamily. We found that MaX1 of *M. acetivorans* is an electrogenic Na^+/Ca^{2+} exchanger with properties most similar to those of mammalian NCX proteins. The similarity is perhaps surprising because homology of NCX and YrbG members is limited to the α repeat motifs. MaX1 is characterized as a Na^+/Ca^{2+} exchanger, as it is able to actively accumulate Ca^{2+} in the presence of a supporting Na^+ gradient. Other ions or energy sources do not seem to have a role in this process. The identification of a prokaryotic Na^+/Ca^{2+} exchanger should provide opportunities for additional structural and functional studies.

Acknowledgments—We thank Jennifer Hsieh and Cheryl Yashar for technical assistance and the UCLA-DOE Protein Expression Core for providing genomic DNA for M. acetivorans.

REFERENCES

1. Philipson, K. D., and Nicoll, D. A. (2000) Sodium/calcium exchange: a molecular perspective. *Annu. Rev. Physiol.* **62,** 111–133
2. Kang, T. M., and Hilgemann, D. W. (2004) Multiple transport modes of the cardiac Na^+/Ca^{2+} exchanger. *Nature* **427,** 544–548
3. Schwarz, E. M., and Benzer, S. (1997) *Calx*, a Na^+/Ca^{2+} exchanger gene of *Drosophila melanogaster*. *Proc. Natl. Acad. Sci. U.S.A.* **94,** 10249–10254
4. Ottolia, M., Nicoll, D. A., and Philipson, K. D. (2005) Mutational analysis of the α-1 repeat of the cardiac Na^+/Ca^{2+} exchanger. *J. Biol. Chem.* **280,** 1061–1069
5. Nicoll, D. A., Hryshko, L. V., Matsuoka, S., Frank, J. S., and Philipson, K. D. (1996) Mutation of amino acid residues in the putative transmembrane segments of the cardiac sarcolemmal Na^+/Ca^{2+} exchanger. *J. Biol. Chem.* **271,** 13385–13391
6. Shigekawa, M., and Iwamoto, T. (2001) Cardiac Na^+/Ca^{2+} exchange: molecular and pharmacological aspects. *Circ. Res.* **88,** 864–876
7. Lytton, J. (2007) Na^+/Ca^{2+} exchangers: three mammalian gene families control Ca^{2+} transport. *Biochem. J.* **406,** 365–382
8. Visser, F., and Lytton, J. (2007) K^+-dependent Na^+/Ca^{2+} exchangers: key contributors to Ca^{2+} signaling. *Physiology* **22,** 185–192
9. Cai, X., and Lytton, J. (2004) The cation/Ca^{2+} exchanger superfamily: phylogenetic analysis and structural implications. *Mol. Biol. Evol.* **21,** 1692–1703
10. Belliveau, J. W., and Lanyi, J. K. (1978) Calcium transport in *Halobacterium halobium* envelope vesicles. *Arch. Biochem. Biophys.* **186,** 98–105
11. Ando, A., Yabuki, M., and Kusaka, I. (1981) Na^+-driven Ca^{2+} transport in alkalophilic *Bacillus*. *Biochim. Biophys. Acta* **640,** 179–184
12. Trombe, M. C. (1993) Characterization of a calcium porter of *Streptococcus pneumoniae* involved in calcium regulation of growth and competence. *J. Gen. Microbiol.* **139,** 433–439
13. Miller, J. H. (1972) *Experiments in Molecular Genetics*, Cold Spring Harbor Laboratory, Cold Spring Harbor, NY
14. Miroux, B., and Walker, J. E. (1996) Overproduction of proteins in *Escherichia coli*: mutant hosts that allow synthesis of some membrane proteins and globular proteins at high levels. *J. Mol. Biol.* **260,** 289–298
15. Hsieh, J. M., Besserer, G. M., Madej, M. G., Bui, H. Q., Kwon, S., and Abramson, J. (2010) Bridging the gap: a GFP-based strategy for overexpression and purification of membrane proteins with intra- and extracellular C termini. *Protein Sci.* **19,** 868–880
16. Nagamori, S., Vázquez-Ibar, J. L., Weinglass, A. B., and Kaback, H. R. (2003) *In vitro* synthesis of lactose permease to probe the mechanism of membrane insertion and folding. *J. Biol. Chem.* **278,** 14820–14826
17. Drew, D., Lerch, M., Kunji, E., Slotboom, D. J., and de Gier, J. W. (2006) Optimization of membrane protein overexpression and purification using GFP fusions. *Nat. Methods* **3,** 303–313
18. Vemuri, R., and Philipson, K. D. (1988) Phospholipid composition modulates the Na^+/Ca^{2+} exchange activity of cardiac sarcolemma in reconstituted vesicles. *Biochim. Biophys. Acta* **937,** 258–268
19. Nicoll, D. A., Ottolia, M., Lu, L., Lu, Y., and Philipson, K. D. (1999) A new topological model of the cardiac sarcolemmal Na^+/Ca^{2+} exchanger. *J. Biol. Chem.* **274,** 910–917
20. Iwamoto, T., Nakamura, T. Y., Pan, Y., Uehara, A., Imanaga, I., and Shigekawa, M. (1999) Unique topology of the internal repeats in the cardiac Na^+/Ca^{2+} exchanger. *FEBS Lett.* **446,** 264–268
21. Sääf, A., Baars, L., and von Heijne, G. (2001) The internal repeats in the Na^+/Ca^{2+} exchanger-related *Escherichia coli* protein YrbG have opposite membrane topologies. *J. Biol. Chem.* **276,** 18905–18907
22. von Heijne, G., and Gavel, Y. (1988) Topogenic signals in integral membrane proteins. *Eur. J. Biochem.* **174,** 671–678
23. Abramson, J., and Wright, E. M. (2009) Structure and function of Na^+ symporters with inverted repeats. *Curr. Opin. Struct. Biol.* **19,** 425–432
24. Li, Z., Nicoll, D. A., Collins, A., Hilgemann, D. W., Filoteo, A. G., Penniston, J. T., Weiss, J. N., Tomich, J. M., and Philipson, K. D. (1991) Identification of a peptide inhibitor of the cardiac sarcolemmal Na^+/Ca^{2+} exchanger. *J. Biol. Chem.* **266,** 1014–1020
25. Matsuoka, S., Nicoll, D. A., Reilly, R. F., Hilgemann, D. W., and Philipson, K. D. (1993) Initial localization of regulatory regions of the cardiac sarcolemmal Na^+/Ca^{2+} exchanger. *Proc. Natl. Acad. Sci. U.S.A.* **90,** 3870–3874
26. Hilge, M., Aelen, J., and Vuister, G. W. (2006) Ca^{2+} regulation in the Na^+/Ca^{2+} exchanger involves two markedly different Ca^{2+} sensors. *Mol. Cell* **22,** 15–25
27. Bers, D. M., Philipson, K. D., and Nishimoto, A. Y. (1980) Sodium/calcium exchange and sidedness of isolated cardiac sarcolemmal vesicles. *Biochim. Biophys. Acta* **601,** 358–371
28. Reeves, J. P., and Sutko, J. L. (1983) Competitive interactions of sodium and calcium with the sodium/calcium exchange system of cardiac sarcolemmal vesicles. *J. Biol. Chem.* **258,** 3178–3182
29. Reeves, J. P., and Hale, C. C. (1984) The stoichiometry of the cardiac sodium/calcium exchange system. *J. Biol. Chem.* **259,** 7733–7739
30. Dong, H., Dunn, J., and Lytton, J. (2002) Stoichiometry of the cardiac

Na^+/Ca^{2+} exchanger NCX1.1 measured in transfected HEK cells. *Biophys. J.* **82,** 1943–1952
31. Philipson, K. D., and Nishimoto, A. Y. (1980) Na^+/Ca^{2+} exchange is affected by membrane potential in cardiac sarcolemmal vesicles. *J. Biol. Chem.* **255,** 6880–6882
32. Hayashi, H., Szászi, K., Coady-Osberg, N., Furuya, W., Bretscher, A. P., Orlowski, J., and Grinstein, S. (2004) Inhibition and redistribution of NHE3, the apical Na^+/H^+ exchanger, by *Clostridium difficile* toxin B. *J. Gen. Physiol.* **123,** 491–504
33. Palty, R., Silverman, W. F., Hershfinkel, M., Caporale, T., Sensi, S. L., Parnis, J., Nolte, C., Fishman, D., Shoshan-Barmatz, V., Herrmann, S., Khananshvili, D., and Sekler, I. (2010) NCLX is an essential component of mitochondrial Na^+/Ca^{2+} exchange. *Proc. Natl. Acad. Sci. U.S.A.* **107,** 436–441
34. Doering, A. E., Nicoll, D. A., Lu, Y., Lu, L., Weiss, J. N., and Philipson, K. D. (1998) Topology of a functionally important region of the cardiac Na^+/Ca^{2+} exchanger. *J. Biol. Chem.* **273,** 778–783
35. Trosper, T. L., and Philipson, K. D. (1983) Effects of divalent and trivalent cations on Na^+/Ca^{2+} exchange in cardiac sarcolemmal vesicles. *Biochim. Biophys. Acta* **731,** 63–68